Nuclear Engineering and Design 244 (2012) 17–24

Contents lists available at SciVerse ScienceDirect

Nuclear Engineering and Design

journal homepage: www.elsevier.com/locate/nucengdes

MAX phase carbides and nitrides: Properties for future nuclear power plant in-core applications and neutron transmutation analysis

E.N. Hoffman[a,*], D.W. Vinson[a], R.L. Sindelar[a], D.J. Tallman[b], G. Kohse[c], M.W. Barsoum[b]

[a] Savannah River National Laboratory, Aiken, SC 29808, United States
[b] Department of Materials Science and Engineering, Drexel University, Philadelphia, PA 19104, United States
[c] Department of Nuclear Engineering, Massachusetts Institute of Technology, Cambridge, MA 02139, United States

ARTICLE INFO

Article history:
Received 23 September 2011
Received in revised form 5 December 2011
Accepted 6 December 2011

ABSTRACT

A family of ternary carbides and nitrides, known as MAX phases, combine attractive properties of both ceramics and metals, and has been suggested for potential nuclear reactor applications. The unirradiated materials properties of importance for in-core structural materials and as fuel pellet coatings for several leading MAX phase materials have been summarized from literature. The materials show high mechanical damage tolerance in terms of creep, thermal/mechanical fatigue and fracture resistance, and very good chemical compatibility with select coolants such as molten lead and sodium. Neutron activation has been calculated for commercial purity materials exposed to both idealized fast and thermal reactor neutron spectra for 10, 30, and 60 years of exposure. The specific activities of Ti_3SiC_2, Ti_3AlC_2, and Ti_2AlC were compared to those of SiC and Alloy 617, two leading candidate materials for next generation reactor components. The specific activities of MAX phases were similar to SiC and three orders of magnitude less than Alloy 617 after 10–60 years decay for all three activation times in both the fast and thermal spectra. As with SiC, the main radioisotopes after a decay period of 10 years for all three activation times in the MAX phases are tritium and C^{14}. Neutron irradiation results of Ti_3SiC_2, Ti_3AlC_2, and Ti_2AlC experimentally confirmed the neutron transmutation analysis.

Published by Elsevier B.V.

1. Introduction

Several next generation nuclear power plant designs require materials to perform at temperatures up to 1000+ °C in fast-neutron environments. The $M_{n+1}AX_n$ (MAX) phases are a new group of layered, machinable, ternary carbides and nitrides, where M is an early transition metal, A is one of elements in groups 13–16, and X is C and/or N. These compounds offer a unique combination of properties, some of which are typical of ceramics, others more typical of metals. As discussed herein, these phases are attractive candidate materials for structural and fuel coating applications at these extreme conditions.

Due to their layered atomic structure and the presence of active basal slip the MAX phases possess unique properties that are atypical for ceramics. The MAX phases are the only known metallically bonded polycrystalline solids to which the description thermodynamically stable nanolaminates applies (Barsoum et al., 1997). Many of the mechanical properties of these materials stem directly from the fact that they are metallically bonded, and basal plane dislocations are mobile, multiply at temperatures as low as 77 K. The latter are arranged either in dislocation pileups or kink boundaries. Single grains can deform by a combination of slip, kink-band formation, and delamination; all dislocation-based (Barsoum et al., 1999; Faber et al., 1999).

Establishing the utility of these materials for in-core nuclear applications requires an evaluation of their neutronics and neutron radiation damage response. A set of unirradiated material properties, important to structural components and fuel pellet coatings, has been assembled as a precursor step to the generation of irradiated properties' data. We also report, for the first time, neutron activation calculations of select commercial purity MAX phases when irradiated in both a fast reactor and thermal reactor neutron spectrum for up to 60 years with up to 10 years decay. These results, benchmarked with a screening irradiation in the Massachusetts Institute of Technology Reactor, provide information on their neutronic performance for in-core applications. Analysis of the results provides an initial assessment of their neutronic performance.

2. Unirradiated materials properties

2.1. Mechanical properties

Some of the MAX phases, such as Ti_3SiC_2, Ti_3AlC_2 and Ti_4AlN_3, in particular, are elastically quite stiff. For example, at 320 GPa, the stiffness of Ti_3SiC_2 is almost three times that of Ti metal, with a

* Corresponding author at: Savannah River Site, 773-A, Aiken, SC 29808, United States. Tel.: +1 803 725 5475; fax: +1 803 725 7369.
E-mail address: Elizabeth.Hoffman@srnl.doe.gov (E.N. Hoffman).

0029-5493/$ – see front matter. Published by Elsevier B.V.
doi:10.1016/j.nucengdes.2011.12.009

similar density of 4.5 g/cm^3 (Barsoum and Radovic, 2004). Ti_3SiC_2 and Ti_2AlC, although elastically stiff, can dissipate up to 25% of the mechanical energy when loaded in compression due to their hysteretic, non-linear elastic behavior, even at room temperatures (Barsoum et al., 2000a; Radovic et al., 2002). The physical mechanism responsible for this non-linear elastic hysteresis is postulated to be the formation and annihilation of dislocation-based incipient kink bands, IKBs. This deformation leads to materials capable of fully reversible non-linear strain, a phenomenon absent in brittle solids. Note that since dislocations are confined to two dimensions, classical work hardening is not possible.

Despite being elastically stiff, these solids are relatively soft, with hardness values between 2 and 8 GPa. The highest value, ≈8 GPa, was measured on Ti_2SiC (Amini et al., 2007). Unlike most traditional ceramics, it is difficult to induce cracks from the corners of Vickers indentations in the MAX phases due to the confinement of the extent of damage to a small zone around the indentation (Pampuch et al., 1993; El-Raghy et al., 1997). The energy-absorbing mechanisms that occur at the indentation corners include diffuse microcracking, delamination, crack deflection, grain push-out and pull-out, and the buckling/kinking of individual grains (El-Raghy et al., 1997).

The fracture toughness of Ti_3SiC_2 is approximately 10 MPa-m$^{1/2}$ at room temperature, and 5 MPa-m$^{1/2}$ at 1200 °C (Gilbert et al., 2000; Chen et al., 2001). The material exhibits stable crack growth or R-curve behavior, with stable crack extension of up to several millimeters with a corresponding toughness of up to approximately 16 MPa-m$^{1/2}$ and 7 MPa-m$^{1/2}$ at room temperature and 1200 °C, respectively (Gilbert et al., 2000; Chen et al., 2001). The high damage tolerance is attributed to kinking and the formation of heavily deformed lamellar bridges in the crack wakes.

Tensile creep studies of Ti_3SiC_2 in the 1000–1200 °C temperature range, showed that the creep resistance is comparable to those of some high temperature metallic alloys (Zhen et al., 2005; Radovic et al., 2003).

The MAX phases, particularly Ti_2AlC, can withstand extreme thermal environments and thermal cycling. The material survived 8000 heating and cooling cycles from room temperature to 1350 °C (Sundberg et al., 2004). The materials also have good thermal shock resistance. Ti_3SiC_2 with a grain size of 100–200 μm quenched from 1400 °C maintained, and in some cases slightly increased, the pre-quench flexural strength (Barsoum, 2000b).

Limited data exists on the MAX phases response to irradiation (Liu et al., 2008; Nappe et al., 2008; Whittle et al., 2010). $Ti_3(Si_{0.95}Al_{0.05})C_2$ and $Ti_3(Si_{0.9}Al_{0.1})C_2$ were irradiated with 75 MeV ^{86}Kr at 20 and 500 °C with heavy ion fluence of 2×10^{11}–10^{15} ion/cm^2. The irradiation at 20 °C showed an increase in hardness with fluence, whereas no significant increase in hardness was seen at 500 °C (Liu et al., 2008). Transmission electron microscope, TEM, examination revealed atomic disorder following exposure of $Ti_3(Si_{0.9}Al_{0.1})C_2$ with 92 MeV Xe to 7.5×10^{18} ion/m^2, at room temperature however, the typical layered structure was preserved (Liu et al., 2010).

2.2. Thermal and electrical properties

Unlike SiC and ZrC, many of the MAX phases are better electrical conductors of electricity than Ti metal (Barsoum, 2006). At ≈30–40 W/m-K, the thermal conductivities of Ti_3SiC_2 and Ti_2AlC at room temperature are also more than double those of pure Ti (Barsoum, 2000b). The MAX phases are good thermal conductors because they are good electrical conductors.

2.3. Chemical stability

Like traditional ceramics, many Al-containing MAX phases are stable in inert atmospheres up to at least 1500 °C; Ti_3SiC_2 is stable up to 2200 °C (Du et al., 2000). However, when exposed at high temperature to oxidizing environments, the MAX phases form oxide scales that depend on their chemistry. For some, like Ti_2AlC, the oxide scales are found to be protective at temperatures as high as 1350 °C for 8000 heating and cooling cycles (Sundberg et al., 2004). The excellent oxidation resistance stems from the formation of a thin tenacious, adherent, alumina layer.

Moreover, Ti_3SiC_2 was found to have excellent corrosion resistance in acid and alkali liquids such as HCl, H_2SO_4, NaOH, and KOH (Jovic and Barsoum, 2004; Jovic et al., 2006a,b). Minimal surface reaction or corrosion has been observed between circulating molten lead and Ti_2AlC and Ti_3AlC_2 at both 650 and 800 °C (Barnes et al., 2008).

2.4. Fabrication

Complex, fully dense, shapes can be fabricated by pressureless sintering of green bodies or by machining from blocks. The MAX phases can be machined using high-speed tool bits with no lubrication or cooling required. Machining is possible due to the fracture of microscopic layers instead of by plastic deformation. Thick films can be produced through traditional thermal spray methods on substrates of aluminum and iron (Frodelius et al., 2008).

3. Neutron activation

Three MAX phases, Ti_3SiC_2, Ti_3AlC_2, and Ti_2AlC, were compared to SiC and Alloy 617, two leading candidates for next generation nuclear power reactors (Shankar and Natesan, 2006; Nanstad et al., 2009; Nozawa et al., 2009; Katoh et al., 2007), in an analysis of neutron activation for exposures to a neutron flux in hypothetical fast and thermal reactors. Activation of materials for reactor internals may challenge waste disposal either at periodic replacement intervals or at the time of reactor decommissioning.

Table 1 lists the nominal commercial-grade material compositions with impurities for the materials considered in the simulation activation. Trace elements were not taken into account in the MAX or SiC calculations. The calculations for the steel included common impurities. The simulated activation was performed using ORIGEN-S of the SCALE code system (SCALE, 2009). ORIGEN-S computes time-dependent concentrations and source terms of radioisotopes, which are simultaneously generated or depleted, through neutronic transmutation, fission, and radiological decay and in-growth. One gram of each subject material was exposed to hypothetical fast reactor and thermal reactor neutron spectra for periods of 10, 30, and 60 years. For the fast reactor spectrum, 238-group cross-sections were collapsed to 1 group using a total neutron flux normalization of the Advanced Breeder Test Reactor spectrum contained in the SCALE system (SCALE, 2009). The total flux assumed for these simulations is 1×10^{15} n/cm^2-s. For the thermal reactor neutron spectrum, continuous energy cross-sections were collapsed to three energy groups from the pointwise energy spectrum for a typical pressurized light water reactor contained in the SCALE system. The three energy groups are a fast group (1–10 MeV) flux of 4.4×10^{13} n/cm^2-s, an epithermal group flux of 1.5×10^{14} n/cm^2-s (1 eV–1 MeV), and a thermal group (0.0–1 eV) of 3.2×10^{13} n/cm^2-s, respectively. Location specific information regarding a collapsed three-group energy distribution was not available as input for the simulations, therefore, engineering judgment was used to estimate the flux profile used in the modeling simulations. The group-average cross-sections were generated by SCALE from the standard ENDF/B-IV libraries.

As noted above, the activation products for each of the materials of interest were determined at exposure intervals of 10, 30,

Table 1
Weight percentage of nominal and impurity elements assumed for the commercial purity materials. The MAX material impurities are based on typical material supplier analyses.

Element	Ti_3SiC_2 (wt%)	Ti_3AlC_2 (wt%)	Ti_2AlC (wt%)	SiC (wt%)	Alloy 617 (wt%)
Ti	73.093	73.510	70.788	0.000	0.3
C	12.277	12.434	9.045	29.950	0.087
O	0.172	0.395	0.487	0.000	0.0
P	0.001	0.001	0.001	0.000	0.00
S	0.001	0.001	0.001	0.000	0.01
Mn	0.007	0.007	0.007	0.000	0.7
Cl	0.007	0.007	0.007	0.000	0.0
N	0.013	0.124	0.173	0.000	0.0
Fe	0.022	0.041	0.048	0.000	1.5
Al	0.007	13.560	19.583	0.000	1.15
Si	14.357	0.007	0.007	70.050	0.5
Mg	0.007	0.007	0.007	0.000	0.0
Na	0.007	0.007	0.007	0.000	0.0
Ni	0.000	0.000	0.000	0.000	52.0
Cr	0.000	0.000	0.000	0.000	22.0
Mo	0.000	0.000	0.000	0.000	9.0
Co	0.000	0.000	0.000	0.000	12.5
Cu	0.000	0.000	0.000	0.000	0.25
B	0.000	0.000	0.000	0.000	0.003

and 60 years. The specific activities of the main radioisotopes, and corresponding specific decay heats, at 0 and 10 years decay times for the materials exposed in the fast reactor, are listed in Tables 2 and 3, respectively. The specific activities of the main radioisotopes, and corresponding specific decay heats, at 0 and 10 years decay times for the materials exposed in the thermal reactor are listed in Tables 4 and 5, respectively.

Specific activities of the activation products, for times up to 10 years at each exposure interval are shown in Figs. 1–3 for the fast reactor exposure, and Figs. 4–6 for the thermal reactor exposure, respectively to the 10-, 30-, and 60-year exposures.

These results clearly show that the total activation of the MAX phases is similar to that of SiC and approximately three orders of magnitude less than Alloy 617 after 10 years of post-exposure

Table 2
Specific activity of primary activation products after decay times of $t = 0$ years and $t = 10$ years following exposure in a fast spectrum reactor. Specific activities are noted in Curies per gram of source material.

10 Year activation				30 Years activation				60 Years activation			
$t = 0$ years		$t = 10$ years		$t = 0$ years		$t = 10$ years		$t = 0$ years		$t = 10$ years	
Iso.	Spec. activity (Ci/g)	Iso.	Spec. activity (Ci/g)	Iso.	Spec. activity (Ci/g)	Iso.	Spec. activity (Ci/g)	Iso.	Spec. activity (Ci/g)	Iso.	Spec. activity (Ci/g)
Ti_3SiC_2											
Al 28	6.0E−02	H 3	6.0E−06	Al 28	6.0E−02	H 3	2.6E−05	Al 28	6.0E−02	H 3	9.7E−05
Sc 47	5.5E−02	C 14	3.8E−06	Sc 47	5.4E−02	C 14	1.1E−05	Sc 47	5.4E−02	C 14	2.2E−05
Sc 46	3.1E−02	Fe 55	3.3E−06	Sc 46	3.1E−02	Fe 55	3.5E−06	Sc 46	3.0E−02	Fe 55	3.4E−06
Sc 48	7.4E−03	Mn 54	1.3E−08	Sc 48	7.4E−03	Mn 54	1.2E−08	Sc 48	7.3E−03	Cl 36	2.4E−08
Ca 45	2.9E−03	Cl 36	4.0E−09	Ca 45	2.9E−03	Cl 36	1.2E−08	Ca 45	2.9E−03	Be 10	1.3E−08
Ti_3AlC_2											
Al 28	1.4E−01	H 3	4.7E−05	Al 28	1.4E−01	H 3	1.3E−04	Al 28	1.4E−01	H 3	2.7E−04
Sc 47	5.5E−02	C 14	3.0E−05	Sc 47	5.5E−02	C 14	8.9E−05	Sc 47	5.4E−02	C 14	1.8E−04
Sc 46	3.1E−02	Fe 55	6.1E−06	Sc 46	3.1E−02	Fe 55	6.5E−06	Sc 46	3.0E−02	Fe 55	6.3E−06
Na 24	8.6E−03	Mn 54	2.3E−08	Na 24	8.6E−03	Mn 54	2.3E−08	Na 24	8.6E−03	Cl 36	2.4E−08
Sc 48	7.5E−03	Cl 36	4.1E−09	Sc 48	7.4E−03	Cl 36	1.2E−08	Sc 48	7.4E−03	Mn 54	2.2E−08
Ti_2AlC											
Al 28	2.0E−01	H 3	6.5E−05	Al 28	2.0E−01	H 3	1.7E−04	Al 28	2.0E−01	H 3	3.3E−04
Sc 47	5.3E−02	C 14	4.1E−05	Sc 47	5.3E−02	C 14	1.2E−04	Sc 47	5.2E−02	C 14	2.4E−04
Sc 46	3.0E−02	Fe 55	7.1E−06	Sc 46	3.0E−02	Fe 55	7.6E−06	Sc 46	2.9E−02	Fe 55	7.5E−06
Na 24	1.3E−02	Mn 54	2.7E−08	Na 24	1.3E−02	Mn 54	2.7E−08	Na 24	1.3E−02	Mn 54	2.6E−08
Sc 48	7.2E−03	Cl 36	3.9E−09	Sc 48	7.2E−03	Cl 36	1.2E−08	Sc 48	7.1E−03	Cl 36	2.3E−08
SiC											
Al 28	2.9E−01	H 3	1.9E−06	Al 28	2.9E−01	H 3	3.2E−05	Al 28	2.9E−01	H 3	1.8E−04
P 32	2.2E−05	C 14	1.7E−06	P 32	6.7E−05	C 14	5.0E−06	H 3	3.2E−04	C 14	9.9E−06
H 3	3.4E−06	Be 10	5.2E−09	H 3	5.6E−05	Be 10	1.6E−08	P 32	1.3E−04	Be 10	3.1E−08
C 14	1.7E−06	P 32	3.3E−10	C 14	5.0E−06	P 32	9.5E−10	C 14	9.9E−06	P 32	1.8E−09
Na 24	9.9E−08	Si 32	3.3E−10	Na 24	3.0E−07	Si 32	9.5E−10	Na 24	6.0E−07	Si 32	1.8E−09
Alloy 617											
Co 58	1.5E+00	Co 60	9.8E−02	Co 58	1.5E+00	Co 60	1.3E−01	Co 58	1.4E+00	Co 60	1.3E−01
Co 60	3.7E−01	Fe 55	6.0E−03	Co 60	4.9E−01	Ni 63	9.3E−03	Co 60	4.9E−01	Ni 63	1.7E−02
Mo 99	2.0E−01	Ni 63	3.3E−03	Mo 99	2.1E−01	Fe 55	6.3E−03	Mo 99	2.1E−01	Fe 55	6.1E−03
Tc 99m	1.8E−01	Ni 59	1.7E−04	Tc 99m	1.9E−01	Ni 59	5.0E−04	Tc 99m	2.0E−01	Ni 59	9.6E−04
Fe 55	7.5E−02	Mo 93	1.6E−04	Fe 55	8.0E−02	Mo 93	4.6E−04	Fe 55	7.7E−02	Mo 93	8.8E−04

Table 3
Specific decay heat from primary activation products after decay times of $t = 0$ years and $t = 10$ years following exposure in a fast spectrum reactor. Specific decay heat is noted in Watts per gram of source material.

10 Year activation				30 Years activation				60 Years activation			
$t = 0$ years		$t = 10$ years		$t = 0$ years		$t = 10$ years		$t = 0$ years		$t = 10$ years	
Iso.	Spec. decay heat (W/g)	Iso.	Spec. decay heat (W/g)	Iso.	Spec. decay heat (W/g)	Iso.	Spec. decay heat (W/g)	Iso.	Spec. decay heat (W/g)	Iso.	Spec. decay heat (W/g)
Ti_3SiC_2											
Al 28	1.1E−03	C 14	1.1E−09	Al 28	1.1E−03	C 14	3.3E−09	Al 28	1.1E−03	C 14	6.6E−09
Sc 46	3.9E−04	H 3	2.0E−10	Sc 46	3.8E−04	H 3	8.7E−10	Sc 46	3.8E−04	H 3	3.3E−09
Sc 48	1.6E−04	Fe 55	1.1E−10	Sc 48	1.6E−04	Fe 55	1.2E−10	Sc 48	1.6E−04	Co 60	1.6E−10
Sc 47	8.8E−05	Mn 54	6.2E−11	Sc 47	8.7E−05	Co 60	6.6E−11	Sc 47	8.7E−05	Fe 55	1.1E−10
Ca 45	1.3E−06	Na 22	2.6E−11	Ca 45	1.3E−06	Mn 54	6.1E−11	Ca 45	1.3E−06	Mn 54	6.0E−11
Ti_3AlC_2											
Al 28	2.5E−03	C 14	8.8E−09	Al 28	2.5E−03	C 14	2.6E−08	Al 28	2.5E−03	C 14	5.1E−08
Sc 46	3.9E−04	H 3	1.6E−09	Sc 46	3.9E−04	H 3	4.2E−09	Sc 46	3.8E−04	H 3	9.2E−09
Na 24	2.4E−04	Fe 55	2.0E−10	Na 24	2.4E−04	Fe 55	2.2E−10	Na 24	2.4E−04	Co 60	2.9E−10
Sc 48	1.6E−04	Mn 54	1.1E−10	Sc 48	1.6E−04	Co 60	1.2E−10	Sc 48	1.6E−04	Fe 55	2.1E−10
Sc 47	8.8E−05	Na 22	2.6E−11	Sc 47	8.8E−05	Mn 54	1.1E−10	Sc 47	8.7E−05	Mn 54	1.1E−10
Ti_2AlC											
Al 28	3.6E−03	C 14	1.2E−08	Al 28	3.6E−03	C 14	3.6E−08	Al 28	3.6E−03	C 14	7.1E−08
Sc 46	3.7E−04	H 3	2.2E−09	Sc 46	3.7E−04	H 3	5.6E−09	Sc 46	3.7E−04	H 3	1.1E−08
Na 24	3.5E−04	Fe 55	2.4E−10	Na 24	3.5E−04	Fe 55	2.5E−10	Na 24	3.5E−04	Co 60	3.5E−10
Sc 48	1.5E−04	Mn 54	1.3E−10	Sc 48	1.5E−04	Co 60	1.4E−10	Sc 48	1.5E−04	Fe 55	2.5E−10
Sc 47	8.5E−05	Co 60	2.7E−11	Sc 47	8.5E−05	Mn 54	1.3E−10	Sc 47	8.4E−05	Mn 54	1.3E−10
SiC											
Al 28	5.3E−03	C 14	4.9E−10	Al 28	5.3E−03	C 14	1.5E−09	Al 28	5.3E−03	H 3	6.1E−09
P 32	9.1E−08	H 3	6.5E−11	P 32	2.8E−07	H 3	1.1E−09	P 32	5.5E−07	C 14	2.9E−09
Na 24	2.8E−09	Be 10	6.2E−12	Na 24	8.3E−09	Be 10	1.9E−11	Na 24	1.7E−08	Be 10	3.7E−11
C 14	4.9E−10	P 32	1.3E−12	H 3	1.9E−09	P 32	3.9E−12	H 3	1.1E−08	P 32	7.6E−12
H 3	1.1E−10	Si 32	1.3E−13	C 14	1.5E−09	Si 32	3.9E−13	C 14	2.9E−09	Si 32	7.5E−13
Alloy 617											
Co 58	8.9E−03	Co 60	1.5E−03	Co 58	8.7E−03	Co 60	2.0E−03	Co 58	8.4E−03	Co 60	2.0E−03
Co 60	5.6E−03	Ni 63	3.4E−07	Co 60	7.5E−03	Ni 63	9.6E−07	Co 60	7.6E−03	Ni 63	1.7E−06
Mo 99	6.5E−04	Fe 55	2.0E−07	Mo 99	6.5E−04	Fe 55	2.1E−07	Mo 99	6.5E−04	Fe 55	2.0E−07
Al 28	2.5E−04	Mo 93	1.5E−08	Al 28	2.5E−04	Nb 93m	4.5E−08	Al 28	2.5E−04	Nb 93m	1.0E−07
Tc 99m	1.6E−04	Nb 93m	1.2E−08	Tc 99m	1.6E−04	Mo 93	4.3E−08	Fe 59	2.3E−04	Mo 93	8.3E−08

decay, irrespective of the activation period for either the fast reactor or the thermal reactor exposure.

The contributions to activity shown in Tables 2 and 4 for the initial discharge, and after a decay period of 10 years show that tritium and C^{14} are the primary radioisotopes in activated Ti_3SiC_2, Ti_3AlC_2, Ti_2AlC and SiC. The primary isotopes in Alloy 617 are Co^{60}, Fe^{55}, and Ni^{63}. These primary radioisotope species are products of multiple step activation of the nominal constituents in the materials. That is, the common impurity species, such as N and O, do not significantly contribute to the activity.

4. Model validation

Small samples of 5 MAX phases, viz. Ti_3SiC_2, Ti_3AlC_2, Ti_2AlC, Ti_2AlN, and Ti_2SC, were exposed in the pneumatic facility designated 2PH1 of the MIT Reactor to assess their activation in preparation for an irradiation campaign to investigate their response to a moderate dose (up to 2 dpa), and moderate temperature (up to 600 °C) irradiation. The 2PH1 facility used for the activation irradiation has a nominal thermal flux of 5.0×10^{13} n/cm^2-s and a nominal fast flux of 1×10^{12} n/cm^2-s

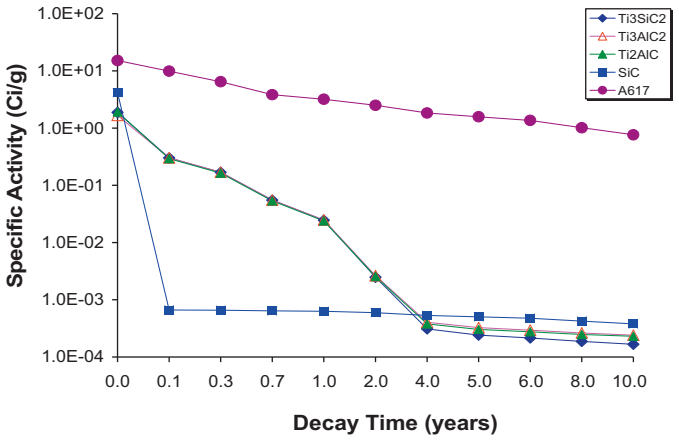

Fig. 1. Radioactive decay based on an activation period of 10 years in a fast reactor for Ti_3SiC_2, Ti_3AlC_2, Ti_2AlC, SiC, and Alloy 617.

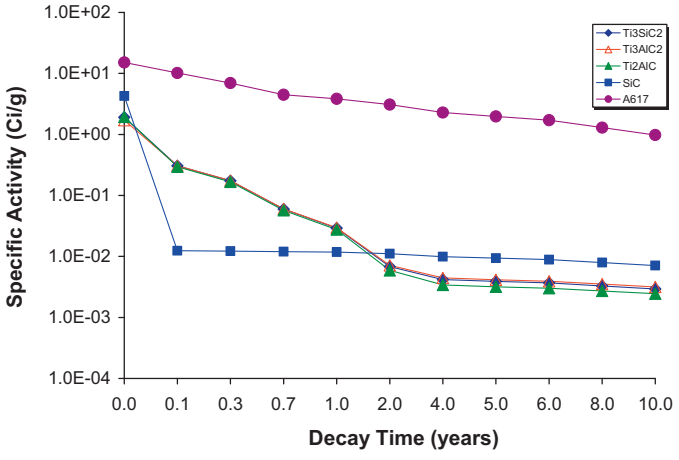

Fig. 2. Radioactive decay based on an activation period of 30 years in a fast reactor for Ti_3SiC_2, Ti_3AlC_2, Ti_2AlC, SiC, and Alloy 617.

Table 4
Specific activity of primary activation products after decay times of t = 0 years and t = 10 years following exposure in a thermal spectrum reactor. Specific Activity is noted in Curies per gram of source material.

10 Year activation				30 Years activation				60 Years activation			
t = 0 years		*t* = 10 years		*t* = 0 years		*t* = 10 years		*t* = 0 years		*t* = 10 years	
Iso.	Spec. activity (Ci/g)	Iso.	Spec. activity (Ci/g)	Iso.	Spec. activity (Ci/g)	Iso.	Spec. activity (Ci/g)	Iso.	Spec. activity (Ci/g)	Iso.	Spec. activity (Ci/g)
Ti_3SiC_2											
Al 28	3.6E−02	Fe 55	1.4E−05	Al 28	3.6E−02	C 14	2.4E−05	Al 28	3.6E−02	H 3	6.0E−05
Sc 47	2.2E−02	C 14	8.3E−06	Sc 47	2.2E−02	Fe 55	1.5E−05	Sc 47	2.2E−02	C 14	4.8E−05
Sc 46	1.7E−02	H 3	1.2E−06	Sc 46	1.7E−02	H 3	1.4E−05	Sc 46	1.7E−02	Fe 55	1.4E−05
Sc 48	3.3E−03	Cl 36	4.7E−07	Sc 48	3.0E−03	Co 60	1.3E−06	Sc 48	2.5E−03	Co 60	3.3E−06
Ca 45	1.2E−03	Co 60	2.8E−07	Ca 45	1.1E−03	Cl 36	9.9E−07	Ca 45	9.3E−04	Cl 36	1.2E−06
Ti_3AlC_2											
Al 28	4.5E−01	C 14	7.7E−05	Al 28	4.5E−01	C 14	2.3E−04	Al 28	4.5E−01	C 14	4.4E−04
Sc 47	2.3E−02	Fe 55	2.6E−05	Sc 47	2.2E−02	Fe 55	2.7E−05	Sc 47	2.2E−02	H 3	6.0E−05
Sc 46	1.7E−02	H 3	1.2E−06	Sc 46	1.7E−02	H 3	1.4E−05	Sc 46	1.7E−02	Fe 55	2.6E−05
Na 24	4.8E−03	Co 60	5.1E−07	Na 24	4.8E−03	Co 60	2.4E−06	Na 24	4.7E−03	Co 60	6.0E−06
Sc 48	3.3E−03	Cl 36	4.7E−07	Sc 48	3.0E−03	Cl 36	9.9E−07	Sc 48	2.5E−03	Cl 36	1.2E−06
Ti_2AlC											
Al 28	6.6E−01	C 14	1.1E−04	Al 28	6.5E−01	C 14	3.2E−04	Al 28	6.5E−01	C 14	6.1E−04
Sc 47	2.2E−02	Fe 55	3.0E−05	Sc 47	2.1E−02	Fe 55	3.2E−05	Sc 47	2.1E−02	H 3	4.4E−05
Sc 46	1.6E−02	H 3	8.8E−07	Sc 46	1.6E−02	H 3	1.0E−05	Sc 46	1.6E−02	Fe 55	3.0E−05
Na 24	6.6E−03	Co 60	6.0E−07	Na 24	6.6E−03	Co 60	2.8E−06	Na 24	6.5E−03	Co 60	7.0E−06
Sc 48	3.2E−03	Cl 36	4.6E−07	Sc 48	2.9E−03	Cl 36	9.5E−07	Sc 48	2.4E−03	Cl 36	1.1E−06
SiC											
Al 28	1.8E−01	H 3	2.9E−06	Al 28	1.8E−01	H 3	3.4E−05	Al 28	1.8E−01	H 3	1.5E−04
P 32	1.5E−04	C 14	2.8E−07	P 32	4.5E−04	C 14	8.5E−07	P 32	8.9E−04	C 14	1.7E−06
H 3	5.1E−06	Be 10	2.3E−09	H 3	5.9E−05	Be 10	7.0E−09	H 3	2.6E−04	Be 10	1.4E−08
C 14	2.8E−07	P 32	1.9E−10	C 14	8.5E−07	P 32	5.8E−10	C 14	1.7E−06	P 32	1.2E−09
Be 10	2.3E−09	Si 32	1.9E−10	p 33	9.3E−09	Si 32	5.8E−10	p 33	4.4E−08	Si 32	1.2E−09
Alloy 617											
Co 60	2.6E+01	Co 60	6.8E+00	Co 60	1.8E+01	Co 60	4.7E+00	Co 60	5.8E+00	Co 60	1.5E+00
Cr 51	9.7E−01	Ni 63	9.1E−02	Cr 51	7.7E−01	Ni 63	2.0E−01	Cr 51	5.4E−01	Ni 63	2.5E−01
Mo 99	2.3E−01	Fe 55	4.0E−03	Mo 99	2.3E−01	Fe 55	4.0E−03	Ni 63	2.7E−01	Fe 55	3.7E−03
Tc 99m	2.0E−01	Ni 59	6.2E−04	Ni 63	2.1E−01	Ni 59	9.2E−04	Mo 99	2.3E−01	Ni 59	8.8E−04
Co 58	1.9E−01	Mo 93	4.2E−05	Tc 99m	2.0E−01	Mo 93	1.1E−04	Tc 99m	2.1E−01	Mo 93	2.0E−04

($E > 1$ MeV) at full power of 4.8 MW. The irradiation for neutron activation was carried out for 6 h, at a position 1 m away from the other samples that were being irradiated to the dose of 2 dpa at an average reactor power of 4.4 MW.

The radioactivity of the exposed samples was then determined by gamma spectrometry. As a validation of the model used to estimate the neutron-induced activation of the materials evaluated in the current work, a simulation of the exposure of the samples with compositions listed in Table 1 was performed. These simulations utilized the collapsed three-group cross sections described previously. For the thermal reactor case, the simulations used an estimated fast group flux of 1×10^{12} n/cm^2-s, an epithermal group flux of 7×10^{12} n/cm^2-s, and a thermal group of 5×10^{13} n/cm^2-s.

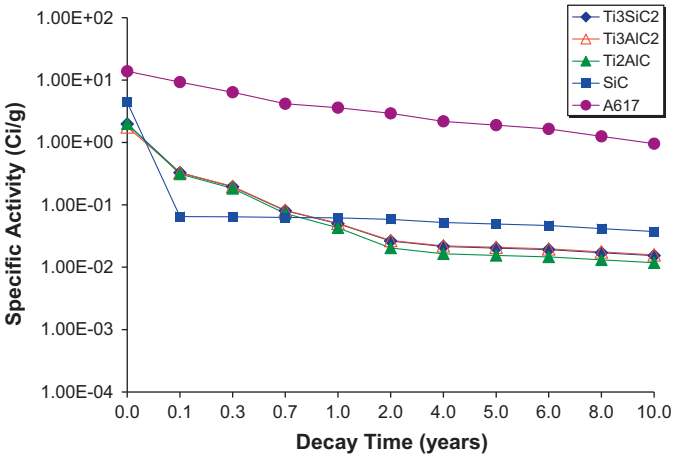

Fig. 3. Radioactive decay based on an activation period of 60 years in a fast reactor for Ti_3SiC_2, Ti_3AlC_2, Ti_2AlC, SiC, and Alloy 617.

Table 6 lists the specific activity of several isotopes generated by the exposure of the five MAX compositions. The table contains both measured values and values estimated by simulated exposure for direct comparison. These data show very good agreement for the specific activity of Sc^{46} that is an activation product of Ti. The disagreement between the results for Cr and Co indicates that trace elements in the exposed samples were not considered in the simulations. The Fe results compare favorably, but the variability in measured results indicates that the differences here may have been introduced by measurement uncertainty. Based upon these observations, it is concluded that the models used in the current work provide reasonable accuracy in predicting the activation of the MAX and other materials.

A separate series of samples with similar composition were irradiated in the MITR core for 42 days at 200 MWd exposure with a neutron flux of 2×10^{13} n/cm^2-s thermal (0–3 keV), 6×10^{13} n/cm^2-s epithermal (3 keV–1 MeV), and 9×10^{13} n/cm^2-s fast (1–20 MeV) in the irradiation of test specimens for material properties. Activation analysis and dose rate measurements were performed on these specimens, approximately 35 days after removal from the reactor. Tantalum 182 was identified following the core irradiation due to the longer time of irradiation, and the relatively large epithermal neutron flux in the core position for its activation. The Ta activity is attributed to Ta impurities in the initial materials with activation

Table 5
Specific decay heat from the primary activation products after decay times of $t = 0$ years and $t = 10$ years following exposure in a thermal spectrum reactor. Specific heat is noted in watts per gram of source material.

10 Year activation				30 Years activation				60 Years activation			
$t = 0$ years		$t = 10$ years		$t = 0$ years		$t = 10$ years		$t = 0$ years		$t = 10$ years	
Iso.	Spec. decay heat (W/g)	Iso.	Spec. decay heat (W/g)	Iso.	Spec. decay heat (W/g)	Iso.	Spec. decay heat (W/g)	Iso.	Spec. decay heat (W/g)	Iso.	Spec. decay heat (W/g)
Ti_3SiC_2											
Al 28	6.5E−04	Co 60	4.3E−09	Al 28	6.5E−04	Co 60	2.0E−08	Al 28	6.5E−04	Co 60	5.0E−08
Sc 46	2.1E−04	C 14	2.4E−09	Sc 46	2.1E−04	C 14	7.2E−09	Sc 46	2.1E−04	C 14	1.4E−08
Sc 48	7.0E−05	Cl 36	6.9E−10	Sc 48	6.3E−05	Cl 36	1.4E−09	Sc 48	5.4E−05	H 3	2.0E−09
Sc 47	3.6E−05	Fe 55	4.7E−10	Sc 47	3.5E−05	Fe 55	5.0E−10	Sc 47	3.5E−05	Cl 36	1.7E−09
Na 24	1.8E−05	H 3	4.0E−11	Na 24	1.8E−05	H 3	4.7E−10	Na 24	1.8E−05	Fe 55	4.7E−10
Ti_3AlC_2											
Al 28	8.1E−03	C 14	2.3E−08	Al 28	8.1E−03	C 14	6.6E−08	Al 28	8.0E−03	C 14	1.3E−07
Sc 46	2.1E−04	Co 60	7.9E−09	Sc 46	2.1E−04	Co 60	3.7E−08	Sc 46	2.1E−04	Co 60	9.2E−08
Na 24	1.3E−04	Fe 55	8.8E−10	Na 24	1.3E−04	Cl 36	1.5E−09	Na 24	1.3E−04	H 3	2.0E−09
Sc 48	7.1E−05	Cl 36	6.9E−10	Sc 48	6.3E−05	Fe 55	9.1E−10	Sc 48	5.4E−05	Cl 36	1.7E−09
Sc 47	3.6E−05	Mn 54	4.1E−11	Sc 47	3.6E−05	H 3	4.7E−10	Sc 47	3.5E−05	Fe 55	8.7E−10
Ti_2AlC											
Al 28	1.2E−02	C 14	3.1E−08	Al 28	1.2E−02	C 14	9.2E−08	Al 28	1.2E−02	C 14	1.8E−07
Sc 46	2.0E−04	Co 60	9.3E−09	Sc 46	2.0E−04	Co 60	4.3E−08	Sc 46	2.0E−04	Co 60	1.1E−07
Na 24	1.8E−04	Fe 55	1.0E−09	Na 24	1.8E−04	Cl 36	1.4E−09	Na 24	1.8E−04	Cl 36	1.7E−09
Sc 48	6.8E−05	Cl 36	6.7E−10	Sc 48	6.1E−05	Fe 55	1.1E−09	Sc 48	5.2E−05	H 3	1.5E−09
Sc 47	3.5E−05	Mn 54	4.9E−11	Sc 47	3.4E−05	H 3	3.4E−10	Sc 47	3.3E−05	Fe 55	1.0E−09
SiC											
Al 28	3.2E−03	H 3	9.8E−11	Al 28	3.1E−03	H 3	1.1E−09	Al 28	3.1E−03	H 3	4.9E−09
P 32	6.1E−07	C 14	8.3E−11	P 32	1.8E−06	C 14	2.5E−10	P 32	3.7E−06	C 14	5.0E−10
H 3	1.7E−10	Be 10	2.8E−12	H 3	2.0E−09	Be 10	8.4E−12	H 3	8.6E−09	Be 10	1.7E−11
C 14	8.3E−11	P 32	7.9E−13	C 14	2.5E−10	P 32	2.4E−12	C 14	5.0E−10	P 32	4.9E−12
Na 24	5.3E−11	Si 32	7.8E−14	Na 24	1.8E−10	Si 32	2.4E−13	Na 24	4.3E−10	Si 32	4.9E−13
Alloy 617											
Co 60	3.9E−01	Co 60	1.1E−01	Co 60	2.7E−01	Co 60	7.3E−02	Co 60	8.9E−02	Co 60	2.4E−02
Co 58	1.1E−03	Ni 63	9.3E−06	Co 58	1.1E−03	Ni 63	2.0E−05	Co 58	9.5E−04	Ni 63	2.6E−05
Mo 99	9.0E−04	Fe 55	1.4E−07	Mo 99	9.1E−04	Fe 55	1.4E−07	Mo 99	9.3E−04	Fe 55	1.3E−07
Al 28	7.1E−04	Ni 59	2.7E−08	Al 28	7.1E−04	Ni 59	4.0E−08	Al 28	7.1E−04	Ni 59	3.9E−08
Cr 51	2.1E−04	Mo 93	4.0E−09	Tc 99m	1.9E−04	Mo 93	1.1E−08	Tc 99m	1.9E−04	Nb 93m	2.2E−08

Table 6
Measured and calculated specific activity of irradiated MAX samples in the pneumatic 2PH1 position.

Material	Activity per sample (Ci/g of source material)							
	Sc 46		Cr 51		Fe 59		Co 60	
	Measured	Calculated	Measured	Calculated	Measured	Calculated	Measured	Calculated
Ti_3SiC_2	7.71E−07	8.60E−07	2.94E−07	2.20E−11	1.97E−08	2.40E−08	0.00E+00	1.05E−17
Ti_2AlC	1.75E−06	8.30E−07	9.23E−07	4.80E−11	2.14E−07	5.20E−08	4.70E−08	2.30E−17
Ti_2AlN	6.86E−07	8.20E−07	5.30E−07	2.14E−11	1.86E−08	2.32E−08	8.51E−09	1.01E−17
Ti_3AlC_2	9.19E−07	8.60E−07	2.26E−07	4.10E−11	0.00E+00	4.40E−08	9.40E−08	1.90E−17
Ti_2SC	1.16E−06	8.00E−07	9.37E−06	2.10E−11	0.00E+00	2.20E−08	1.80E−06	9.80E−18

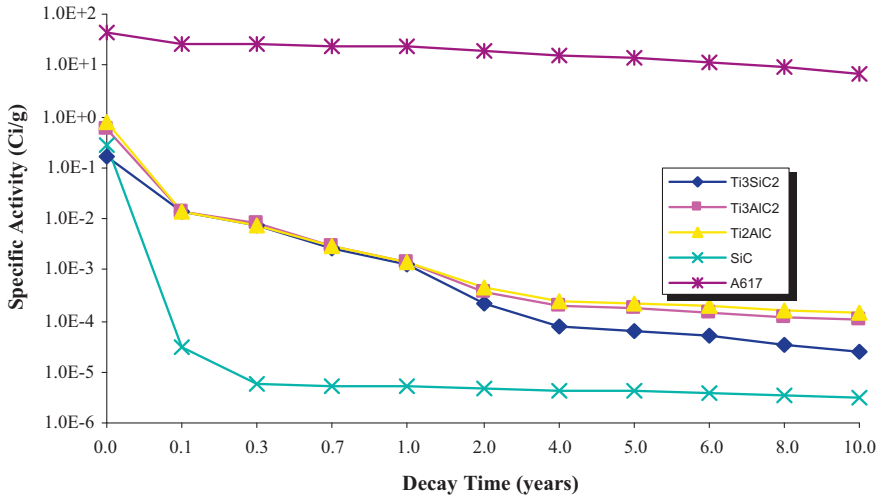

Fig. 4. Radioactive decay based on an activation period of 10 years in a thermal reactor for Ti_3SiC_2, Ti_3AlC_2, Ti_2AlC, SiC, and Alloy 617.

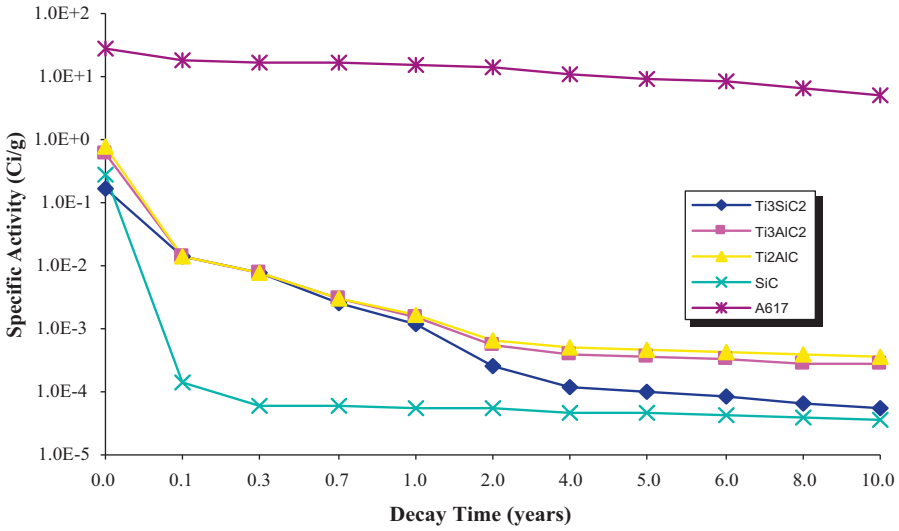

Fig. 5. Radioactive decay based on an activation period of 30 years in a thermal reactor for Ti_3SiC_2, Ti_3AlC_2, Ti_2AlC, SiC, and Alloy 617.

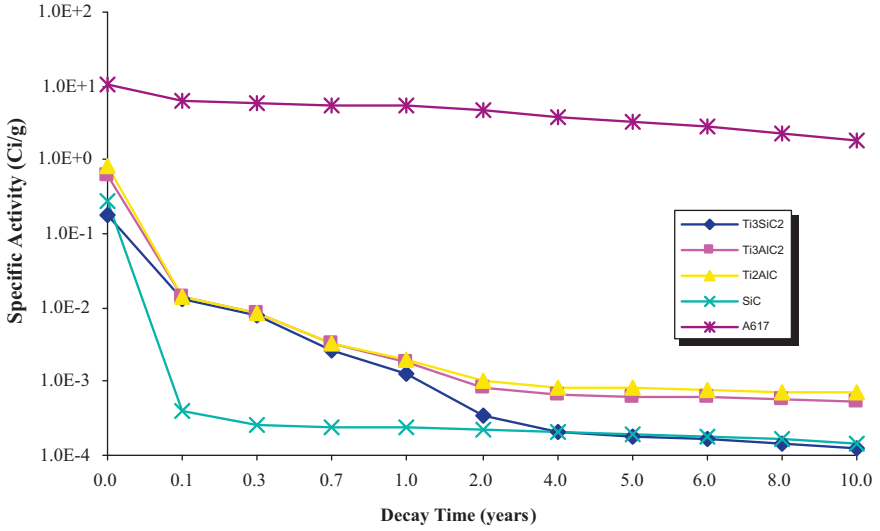

Fig. 6. Radioactive decay based on an activation period of 60 years in a thermal reactor for Ti_3SiC_2, Ti_3AlC_2, Ti_2AlC, SiC, and Alloy 617.

through the reaction $Ta^{181}(n,\gamma)Ta^{182}$. In the Ti_2SC material, the Ta levels are high enough to also see Hf^{181}, which is produced by a fast neutron (n,p) reaction on Ta.

5. Summary and conclusions

The mechanical properties and fabricability of the MAX phases render them good candidates for advanced nuclear reactor, high-temperature applications. Neutron damage studies are needed, and are in progress, to provide empirical data to assess their effect on properties for in-core applications.

Activation calculations using the nominal, and common impurity elements show that the MAX phases are similar to SiC in total activity after an exposure of up to 60 years and a decay period of several years. Specifically, the materials were exposed to both idealized fast and thermal reactor neutron spectra for 10, 30, and 60 years of exposure. The specific activities of Ti_3SiC_2, Ti_3AlC_2, and Ti_2AlC were compared to those of SiC and Alloy 617, two leading candidate materials for next generation reactor components. The specific activities of these MAX phases were similar to SiC and three orders of magnitude less than Alloy 617 after 10–60 years decay for all three activation times in both the fast and thermal spectra. As with SiC, the main radioisotopes after a decay period of 10 years for all three activation times in the MAX phases are tritium and C^{14}. Neutron irradiation results of Ti_3SiC_2, Ti_3AlC_2, and Ti_2AlC experimentally confirmed the neutron transmutation analysis.

References

Amini, S., et al., 2007. J. Am. Ceram. Soc. 90 (12), 3953.
Barnes, L.A., et al., 2008. J. Nucl. Mater. 373, 424.
Barsoum, M.W., 2000b. Prog. Solid State Chem. 28, 201.
Barsoum, M.W., 2006. In: Buschow, K.H.J., et al. (Eds.), Encyclopedia of Materials Science and Technology. Elsevier, Amsterdam.
Barsoum, M.W., Radovic, M., 2004. In: Buschow, K.H.J., et al. (Eds.), Enc. Mat. Sci. Tech. Elsevier, Amsterdam.
Barsoum, M.W., et al., 1997. Scr. Metall. Mater. 36, 535.
Barsoum, M.W., et al., 1999. Metall. Mater. Trans. 30A, 1727.
Barsoum, M.W., et al., 2000a. Metall. Mater. Trans. 31A, 1857.
Chen, D., et al., 2001. J. Am. Ceram. Soc. 84, 2914.
Du, Y., et al., 2000. J. Am. Ceram. Soc. 83 (1), 197.
El-Raghy, T., et al., 1997. J. Am. Ceram. Soc. 80, 513.
Faber, L., et al., 1999. Philos. Mag. Lett. 79, 163.

Frodelius, J., et al., 2008. Surf. Coat. Technol. 202, 5976.
Gilbert, C.J., et al., 2000. Scr. Mater. 42, 761.
Jovic, V.D., Barsoum, M.W., 2004. J. Electrochem. Soc. 151, B71.
Jovic, V.D., et al., 2006a. J. Electrochem. Soc. B238–B243, 153.
Jovic, V.D., et al., 2006b. Corros. Sci. 48, 4274.
Katoh, Y., et al., 2007. J. Nucl. Mater. 367–370, 659.
Liu, X., et al., 2008. TEM observations and nanoindentation measurements of Ti_3SiC_2 irradiated by charged particles. In: CIMTEC, Verona, Italy.
Liu, X.M., et al., 2010. J. Nucl. Mater. 401, 149.
Nanstad, R.K., et al., 2009. J. Nucl. Mater. 392 (2), 331.
Nappe, J.C., et al., 2008. Study of the irradiation damages in Ti_3SiC_2. In: E-MRS Spring Meeting, Strasbourg, Germany.
Nozawa, T., et al., 2009. J. Nucl. Mater. 386–388, 622.
Pampuch, R., et al., 1993. J. Mater. Synth. Process. 1, 93.
Radovic, M., et al., 2002. Acta Mater. 50, 1297.
Radovic, M., et al., 2003. J. Alloys Compd. 361, 299.
SCALE: A Modular Code System for Performing Standardized Computer Analyses for Licensing Evaluation, 2009.
Shankar, P.S., Natesan, K., 2006. J. Nucl. Mater. 366, 28.
Sundberg, M., et al., 2004. Ceram. Int. 30, 1899.
Whittle, K.R., et al., 2010. Radiation tolerance of $M_{N+1}AX_N$ phases, Ti_3AlC_2 and Ti_3SiC_2. Acta Mater. 58, 4362.
Zhen, T., et al., 2005. Acta Mater. 53, 4963.